Mathematical modeling of scaling-free membrane module by combining residence time distribution, metastability, and induction time

Marian Turek[a], Krzysztof Piotrowski[b,*], Piotr Dydo[a], Krzysztof Mitko[a], Ewa Laskowska[a], Agata Jakóbik-Kolon[a]

[a]*Faculty of Chemistry, Department of Inorganic, Analytical Chemistry and Electrochemistry, Silesian University of Technology, B. Krzywoustego 6, 44-100 Gliwice, Poland, Tel./Fax: (+4832) 2371383, 2372277; email: marian.turek@polsl.pl (M. Turek)*
[b]*Faculty of Chemistry, Department of Chemical Engineering and Process Design, Silesian University of Technology, M. Strzody 7, 44–101 Gliwice, Poland, Tel./Fax: (+4832) 2371461; email: krzysztof.piotrowski@polsl.pl*

ABSTRACT

In highly concentrated solutions, with complex ionic composition, the nuclei formation and their surface deposition/growth might result in a severe membrane scaling risk and limit their efficiency. Some scaling prevention techniques exist which are based on correction in feedwater composition and/or antiscalant addition, affecting either ionic equilibriums or sparingly soluble salts formation (nucleation, crystal growth, and deposition). Contrary, a different approach seems to be rational. It includes specific physical aspects of the scaling-underlying phenomena. The idea is based on the identification of the scaling-free operating conditions by adjusting the time required for the ions to pass through RO module with nucleation induction times (metastability) of the potential scalants. Stable performance of the membrane module may be possible without any antiscalants addition. Analysis of membrane modules, of different residence time distributions (effect of spacers geometry and flow rate), was done. The authors' own experimental data concerning the maximal attainable supersaturation C_{max} of $CaSO_4$ for different dC/dt and NaCl concentrations (C_{NaCl}), were coupled with literature data of induction time t_{ind} in these systems. As a result simulation of membrane safe work scenarios with the identification of the operational limits was possible. Some economically optimal exploitation strategies and practical design rules were suggested.

Keywords: Scaling; Residence time distribution; Metastable zone; Induction time; Nucleation

1. Introduction

Membrane processes, because of their simple operation principle, are commonly used in various separation technologies. However, in highly concentrated solutions, with complex composition, formation of inorganic salts nuclei, and their growth might induce severe scaling risk and limit water recovery [1–10]. To avoid this some scaling prevention techniques were proposed. These are mainly based on correction in feedwater composition and/or antiscalant addition to feedwater that affects either equilibrium of sparingly soluble salts formation (like $CaSO_4$ or $CaCO_3$) or modifies their nucleation, crystal growth, and deposition rates. Contrary, we propose a different approach; we believe one should focus on specific physical aspects of the

* Corresponding author.

scaling-underlying phenomena and identify the scaling-free operating conditions by analyzing of the time required for the salt molecules to pass through the RO module with nucleation induction times (metastability) [11–13]. When transportation of the systematically concentrating liquid through the membrane module will be faster than the time necessary for the accumulation of the concentration up to upper metastability limits and induction time representing the delay in spontaneous discharging of the accumulated solute – spontaneous nucleation in membrane unit will be effectively prevented. Stable operation of the membrane system is, however, possible without any antiscalants consumption. Nevertheless, to effectively and possibly precisely predict the system performance some crucial information about the metastable zone width of potentially precipitating compounds (dependent on concentrating rate dC/dt, feed composition, etc.) and their induction times is necessary.

2. Simulated object and models

The comparative analysis of various membrane unit constructions, characterized by different residence time distribution profiles, was done [14–16]. The residence time distribution characteristics resulted from different flow conditions, being affected not only by the volumetric flow rate of the processed liquid, but also by the geometry of the unit spacers. The authors' laboratory data covering maximal attainable supersaturation C_{max} of calcium sulfate $CaSO_4$ for different concentrating rates dC/dt and at various NaCl concentrations (C_{NaCl}) [17], mathematically elaborated as the $C_{max} = f(dC/dt, C_{NaCl})$, $C^* = f(C_{NaCl})$ were employed together with general literature equation form for the induction time t_{ind} estimation in such systems [12] for the simulation of each membrane unit's safe work scenarios ($t_{ind} = f(C_{out}, C^*)$) with their critical discussion. The calcium sulfate/sodium chloride system was used for the simulation considering its practical significance in membrane processes. For each membrane unit's construction the operational limits were identified, compared, as well as recommendations concerning the possible corrections of working conditions for optimal membrane operation strategies – rational choosing of optimal final outlet concentration $C_{out} = f(C_{max})$ – were proposed and explained. These are based not only on the restrictions concerning C_{max}, but must also consider complex nonlinear interdependencies and feedbacks between $t_{ind} = f(C_{out}, C^*)$, where $C_{out} = f(C_{max})$, $C^* = f(C_{NaCl})$, and while $C_{max} = f(dC/dt, C_{NaCl})$.

Thus, the induction time t_{ind} depends on the selected outlet supersaturation C_{out}, which is dependent on the Designer's decision taking into account, among others, the maximum value of supersaturation, which – in turn – depends on the concentration rate dC/dt and concentration of NaCl co-present in this particular (here – model) solution.

Considering the whole technological process of retentate concentration in a membrane module, the following stages can be conventionally separated together with their conventional process times:

- concentration of the solution from the inlet value C_{in} up to lower boundary of the metastable zone C_{LBMZ} ($=C^*$) (within undersaturation area) – time 1,

- further concentration of the solution from the value C_{LBMZ} ($=C^*$) up to the final retentate concentration (= termination of the concentration process), C_{out} (within metastable zone) – time 2,

- removal of the supersaturated (but still metastable) solution from the membrane module without further modification of its concentration C_{out} – time 3, thus the sequence of events may be described mathematically in the following formula of the conventional "process/residence time balance," Eq. (1):

$$\left[\frac{C_{LBMZ}-C_{in}}{\frac{dC}{dt}}\right]+\left[\frac{C_{out}-C_{LBMZ}}{\frac{dC}{dt}}\right]+\left[t_{ind}\left(C_{out}\right)\right] > \tau_{99\%} = \tau + 3\sigma$$

$$\left[\text{time 1}\right] + \left[\text{time 2}\right] + \left[\text{time 3}\right] > \tau_{99\%} = \tau + 3\sigma$$

(1)

where C_{LBMZ} ($=C^*$) – concentration of retentate representing lower boundary of the metastable zone, C_{in} – inlet concentration of the feed (at module inlet), C_{out} – final concentration of retentate (termination of membrane process), dC/dt – concentrating (supersaturating) rate resulting from the membrane process intensity, t_{ind} – induction time (correlated with C_{out}), $\tau_{99\%}$ – residence time corresponding to removal of 99% of the feed from working volume of the membrane module, τ – mean residence time of retentate in a working volume of the membrane module, and σ – standard deviation.

Of course, equally important and necessary condition for the scaling/nucleation phenomena prevention according to the presented concept is that final (outlet) retentate concentration $C_{out} < C_{UBMZ}$ representing the upper boundary of the metastable zone, thus labile region boundary (further denoted as C_{max}).

2.1. Simulated object

The membrane module in electrodialyzer, of effective membrane length 42 and of 2 cm channel width, described in detail in Turek and Mitko [14], was assumed as the simulated object. For this object residence times, depending on the assumed process conditions, varied within the ($\tau = 82 \pm 3$ s, $\sigma^2 = 1{,}486 \pm 253$ s²) – ($\tau = 144 \pm 7$ s, $\sigma^2 = 8{,}266 \pm 1{,}575$ s²) range.

2.2. Maximal supersaturation

Calculations involved dependency of maximal supersaturation (C_{max}) on concentrating rate dC/dt (directly representing the membrane process efficiency) and concentration of co-present NaCl (C_{NaCl}). The following general model frame, Eq. (2) [17] was used:

$$\ln\left(\frac{dC}{dt}\right) = \ln k_N + a\frac{1}{\ln^2\left(S_{crit}\right)}$$

(2)

However, for the simulation purposes, Eq. (2) was further transformed into a more convenient form of Eq. (2a) making direct calculation of C_{max} possible:

$$\exp\left[\sqrt{\dfrac{a}{\ln\left(\dfrac{dC}{dt}\right)-\ln k_N}}\right]=S_{\mathrm{crit}}=\dfrac{C_{\max}}{C^*} \tag{2a}$$

Based on the authors' own set of experimental data [17] the following correlation for $a = f(C_{\mathrm{NaCl}})$, Eq. (3) was proposed valid for C_{NaCl} = 0.4–2.0 mol/dm³, with standard error 0.1107 and R^2 0.966:

$$a = -3.3820 + 1.6543 \cdot C_{\mathrm{NaCl}} - 0.5268 \cdot C_{\mathrm{NaCl}}^2 \tag{3}$$

For k_N parameter, considering its nearly constant value, mean value of k_N = 2.38 was assumed [17].

2.3. Induction time

For the calculation of induction time in the simulated process environment the following general model frame, Eq. (4), was used [9,18–32]:

$$t_{\mathrm{ind}}\left(C_{\mathrm{out}}, C^*\right) = t_{\mathrm{ind}}\left(C_{\mathrm{out}}, C_{\mathrm{NaCl}}\right) = \dfrac{1.3 \cdot 10^5}{S^{5.6}} = \dfrac{1.3 \cdot 10^5}{\left(\dfrac{C_{\mathrm{out}}}{C^*}\right)^{5.6}} \tag{4}$$

2.4. Saturation concentration of $CaSO_4$, C^*, depending on NaCl concentration

The following relations, Eqs. (5)–(7), were mathematically elaborated based on the available in literature data concerning the solubility of $CaSO_4$, C^*, depending on the NaCl additive concentration co-present in the processed solution, C_{NaCl}:

$$C^* = \dfrac{0.0126 + 0.1342 \cdot C_{\mathrm{NaCl}}}{1 + 2.2976 \cdot C_{\mathrm{NaCl}} - 0.0444 \cdot C_{\mathrm{NaCl}}^2} \tag{5}$$

valid for: C_{NaCl} = 0–2 mol/dm³, standard error 0.00033, R^2 0.999 [17]:

$$C^* = \dfrac{0.0124 - 0.0381 \cdot C_{\mathrm{NaCl}}}{1 - 8.9648 \cdot C_{\mathrm{NaCl}} + 26.1254 \cdot C_{\mathrm{NaCl}}^2} \tag{6}$$

valid for: C_{NaCl} = 0–0.173 mol/dm³, standard error 0.00047, R^2 0.996 [33], as well as:

$$C^* = \dfrac{0.0147 + 0.0369 \cdot C_{\mathrm{NaCl}}}{1 + 0.1435 \cdot C_{\mathrm{NaCl}} + 0.1456 \cdot C_{\mathrm{NaCl}}^2} \tag{7}$$

valid for: C_{NaCl} = 0–5.4 mol/dm³, standard error 0.00167, R^2 0.993 [34].

3. Simulations

For the practical technological process simulations the following two working equations, Eqs (8)–(9), derived based on the presented earlier Eqs. (2a) and (3)–(5) were coupled:

$$C_{\max}\left(\dfrac{dC}{dt}, C_{\mathrm{NaCl}}\right) = \exp\left[\sqrt{\dfrac{a}{\ln\left(\dfrac{dC}{dt}\right)-\ln k_N}}\right] \cdot C^*$$

$$= \exp\left[\sqrt{\dfrac{-3.3820 + 1.6543 \cdot C_{\mathrm{NaCl}} - 0.5268 \cdot C_{\mathrm{NaCl}}^2}{\ln\left(\dfrac{dC}{dt}\right) - 2.38}}\right] \cdot \tag{8}$$

$$\left(\dfrac{0.0126 + 0.1342 \cdot C_{\mathrm{NaCl}}}{1 + 2.2976 \cdot C_{\mathrm{NaCl}} - 0.0444 \cdot C_{\mathrm{NaCl}}^2}\right)$$

$$t_{\mathrm{ind}}\left(C_{\mathrm{out}}, C_{\mathrm{NaCl}}\right) = \dfrac{1.3 \cdot 10^5}{S^{5.6}} = 1.3 \cdot 10^5 \cdot \tag{9}$$

$$\left(\dfrac{C_{\mathrm{out}}}{\dfrac{0.0126 + 0.1342 \cdot C_{\mathrm{NaCl}}}{1 + 2.2976 \cdot C_{\mathrm{NaCl}} - 0.0444 \cdot C_{\mathrm{NaCl}}^2}}\right)^{-5.6}$$

Simulations were done for the following parameter ranges:

- dC/dt = 0.1–1 mol/(dm³ h) (for simplification constant, given concentrating rate was assumed in each simulation),
- C_{NaCl} = 0–2 mol/dm³.

Simultaneous, direct effect of concentrating rate dC/dt in the module (representing the intensity of the membrane process) and C_{NaCl} (partly representing the chemical composition of the retentate) on the maximal attainable concentration $C_{\max}$, representing thus upper metastability limit, is presented in Fig. 1. In Fig. 2, however, effect of dC/dt and
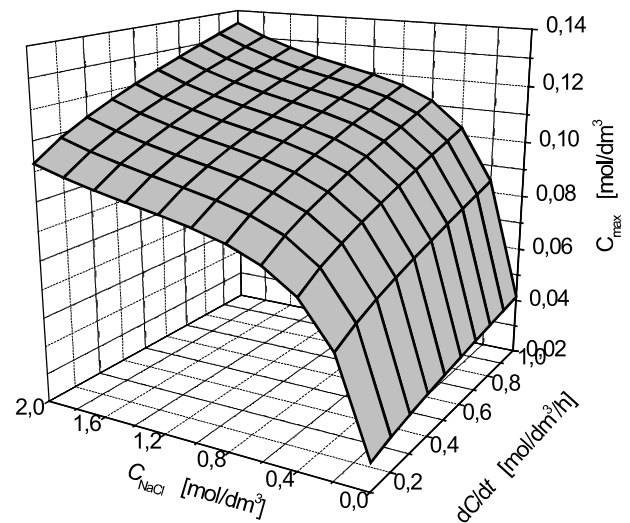

Fig. 1. Maximal concentration $C_{\max}$ of supersaturated $CaSO_4$ solution (upper boundary of the metastable zone) depending on concentrating rate dC/dt arranged in membrane module and concentration of NaCl, C_{NaCl} (graphical projection of Eq. (8)).
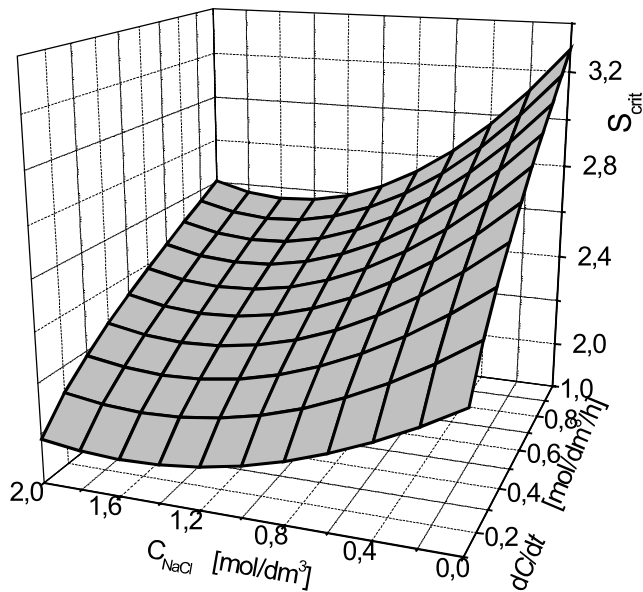
Fig. 2. Maximal (critical) relative supersaturation $S_{crit} = C_{max}/C^*$ of supersaturated $CaSO_4$ (upper boundary of the metastable zone) depending on concentrating rate dC/dt arranged in a membrane module and concentration of NaCl, C_{NaCl} (graphical projection of Eq. (8)).
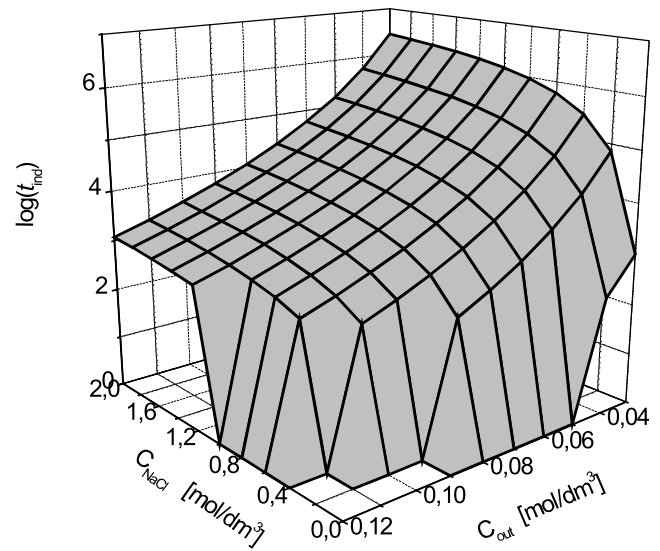

Fig. 3. Induction time ($\log(t_{ind})$) in a supersaturated aqueous solutions of $CaSO_4$ (within the metastable zone) as the function of the assumed final retentate concentration C_{out} and concentration of NaCl, C_{NaCl} (C_{out} = 0.03–0.12 mol/dm³, C_{NaCl} = 0–2 mol/dm³).
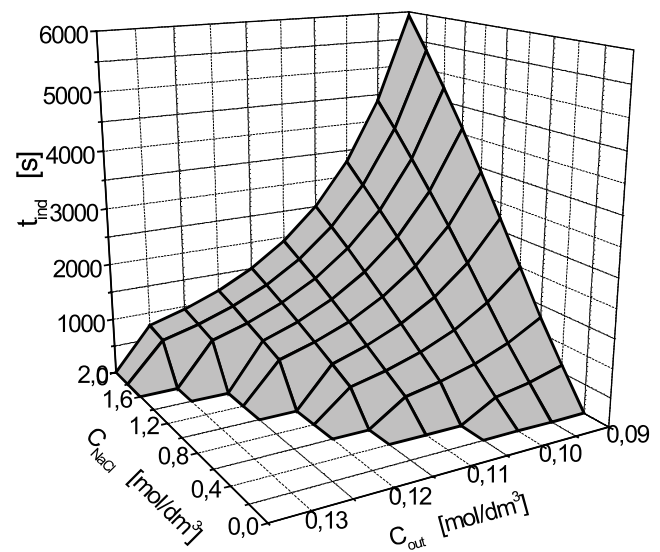

Fig. 4. Induction time t_{ind} in supersaturated aqueous solutions of $CaSO_4$ (within the metastable zone) as the function of the assumed final retentate concentration C_{out} and concentration of NaCl C_{NaCl} (C_{out} = 0.09–0.135 mol/dm³, C_{NaCl} = 0–2 mol/dm³).

C_{NaCl} combination on $S_{crit} = C_{max}/C^*$ is presented, representing net effect of two complex dependencies: $C_{max} = f(dC/dt, C_{NaCl})$, Eq. (8) and $C^* = f(C_{NaCl})$, Eq. (5). In Figs. 3 and 4, strongly non-linear effects of final retentate concentration C_{out} and concentration of co-present NaCl (C_{NaCl}) combinations on the resulting induction times ($\log(t_{ind})$ – Fig. 3, t_{ind} – Fig. 4) are demonstrated.

To demonstrate the authors' concept of the safe membrane work conditions closer, some simulations of the membrane module work under various exemplary process conditions are presented. In Table 1, design calculations of membrane module performance (design assumptions: $\tau_{99\%}$ = 1,000 s, from which only 384 s is dedicated for section (A) – working membrane range [14]) are demonstrated – effect of the main process parameter dC/dt on the final process effects: C_{out} and corresponding $t_{ind}(C_{out})$. Exemplary feed composition: C_{in} = 0.01 mol $CaSO_4/dm^3$, C_{NaCl} = 0.22 mol/dm³ was considered. In Table 2 similar simulation of the membrane process is presented, but in this case – representing different process conditions resulting from, for example, different construction of the spacers arrangement, different working part's length, the different flow rate of retentate, and hydrodynamic flow conditions – the residence time is $\tau_{99\%}$ = 500 s (from which only 198 s is dedicated for the section (A) – working membrane range [14]).

To clearly present the authors' idea, spatial data arrangement from Tables 1 and 2 are presented in Fig. 5 and in Fig. 6.

4. Discussion

In general, the final concentration of retentate should be within the metastable region of the processed solution,

$C^* < C_{out} < C_{max}$. Considering the idea of safe working conditions recommended for membrane module (scaling prevention), the final concentration of retentate should be deeply below C_{max}, which – being the upper boundary of the metastable zone – corresponds to instant spontaneous nucleation (labile range beginning). On the other hand, significant devaluation of C_{out}, providing scaling prevention, maybe not economical since intensive concentrating of the feed is usually demanded. Some compromise is thus required, however, based on reliable simulation/prediction methodology.

Table 1
Simulation of the membrane concentrating process in an aqueous solution of $CaSO_4$ (with the co-presence of NaCl) in a membrane module characterized by $\tau_{99\%}$ = 1,000 s (from which the initial 384 s is dedicated for the section (*A*) – working membrane range)

No.	C_{in} mol/dm³	C_{NaCl} mol/dm³	dC/dt mol/(dm³h)	C_{out} mol/dm³	C_{max} mol/dm³	C_{out}/C_{max} %	t_{ind} s	Maximal permissible residence time (384 s + t_{ind}), s
1			0.1	0.0207	0.0627	32.94	Undersaturated	–
2			0.2	0.0313	0.0671	46.69	69,531	69,915
3			0.3	0.0420	0.0704	59.64	13,478	13,862
4			0.4	0.0527	0.0732	71.90	3,795	4,179
5			0.5	0.0633	0.0758	83.55	1,351	1,735
6			0.6	0.0740	0.0782	94.65	565	949
7			0.7	0.0847	0.0804	105.25	0	–
8			0.8	0.0953	0.0826	115.39	0	–
9			0.9	0.1060	0.0847	125.09	0	–
10	0.01	0.22	1.0	0.1167	0.0868	134.39	0	–
			Suggested improvement – shorter concentrating time in a membrane module, *t* = 310 s					
7a			0.7	0.0703	0.0804	87.37	754	1,064
			Suggested improvement – shorter concentrating time in a membrane module, *t* = 270 s					
8a			0.8	0.0700	0.0826	84.73	771	1,041
			Suggested improvement – shorter concentrating time in a membrane module, *t* = 230 s					
9a			0.9	0.0675	0.0847	79.66	946	1,176
			Suggested improvement – shorter concentrating time in a membrane module, *t* = 210 s					
10a			1.0	0.0683	0.0868	78.71	883	1,093

C^* = 0.028 mol/dm³

Table 2
Simulation of the membrane concentrating process in an aqueous solution of $CaSO_4$ with the co-presence of NaCl in a membrane module characterized by $\tau_{99\%}$ = 500 s (from which the initial 198 s is dedicated for the section (*A*) – working membrane range)

No.	C_{in} mol/dm³	C_{NaCl} mol/dm³	dC/dt mol/(dm³h)	C_{out} mol/dm³	C_{max} mol/dm³	C_{out}/C_{max} %	t_{ind} s	Maximal permissible residence time, s
1			0.1	0.0155	0.0627	24.70	Undersaturated	–
2			0.2	0.0210	0.0671	31.29	Undersaturated	–
3			0.3	0.0265	0.0704	37.63	Undersaturated	–
4			0.4	0.0320	0.0732	43.69	61,798	61,996
5	0.01	0.22	0.5	0.0375	0.0758	49.47	25,424	25,622
6			0.6	0.0430	0.0782	55.00	11,814	12,012
7			0.7	0.0485	0.0804	60.29	6,021	6,219
8			0.8	0.0540	0.0826	65.36	3,299	3,497
9			0.9	0.0595	0.0847	70.22	1,917	2,115
10			1.0	0.0650	0.0868	74.87	1,168	1,366

C^* = 0.028 mol/dm³

Comparing Figs. 1 and 2 one can notice, that C_{max} increases with C_{NaCl} increase. Especially strong, non-linear dependency is observed within the C_{NaCl} 0–0.6 mol/dm³ range. The effect of concentrating rate dC/dt on C_{max} is also visible, but it is less significant. Considering the effect of C_{NaCl} raise on S_{crit} = C_{max}/C^* one observes some decreasing trend, however with the distinct, shallow minimum. This is a manifestation of $C^* = f(C_{NaCl})$ dependency contribution, with its own intrinsic non-linearity (Eqs. (5) and (8)).

The effect of final retentate concentration, C_{out}, and NaCl concentration, C_{NaCl}, on induction time was presented in Figs. 3 and 4. Since in Fig. 3, the semi-logarithmic coordinates are used, the $\log(t_{ind}) = f(C_{out}, C_{NaCl})$ may be projected for broader C_{out} range (0.03–0.12 mol/dm³), where very high values of t_{ind} and even of $\log(t_{ind})$ are observed, especially for smaller C_{out} values. Contrary, in Fig. 4, the $t_{ind} = f(C_{out}, C_{NaCl})$ dependency in narrower C_{out} range is demonstrated, where – because of higher C_{out} thus shorter resulting induction times – these t_{ind} values with significant non-linearity can be presented directly.

In the further calculations there was assumed, that concentrating rate dC/dt is a fully independent design
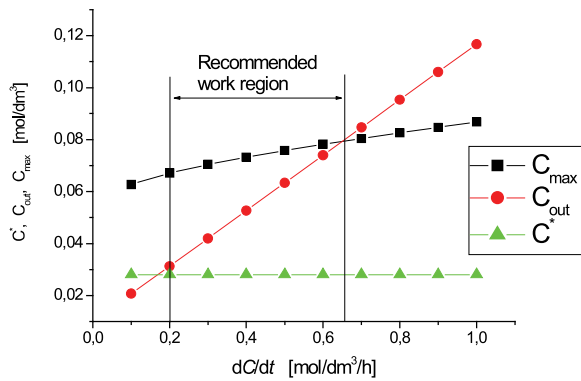
Fig. 5. Effect of the membrane process intensity (represented by concentrating rate dC/dt = 0.1–1.0 mol/(dm³ h)) on the outlet concentration of retentate C_{out} and the maximal attainable concentration of the retentate C_{max} (saturation concentration C^* added as the reference) ($\tau_{99\%}$ = 1,000 s where the initial 384 s is attributed to the working membrane range, data from Table 1).
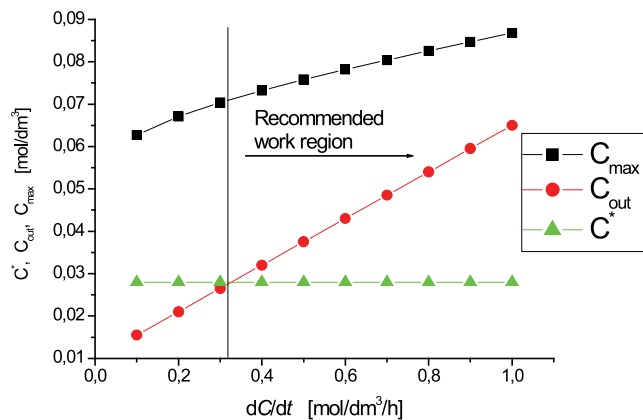

Fig. 6. Effect of the membrane process intensity (represented by concentrating rate dC/dt = 0.1–1.0 mol/(dm³ h)) on the outlet concentration of retentate C_{out} and on the maximal attainable concentration of the retentate C_{max} (saturation concentration C^* added as the reference) ($\tau_{99\%}$ = 500 s where the initial 198 s is attributed to the working membrane range, data from Table 2).

variable. Moreover, for the simplification of exemplary calculations flow through working membrane section (*A*) is approximated by ideal plug-flow, while the outlet section of module (*B*) is assumed to represent some sub-volume with its intrinsic residence time distribution. However, flow through the whole membrane modulus (*A* + *B*) represents thus some resulting residence time distribution.

In Table 1, there are presented some data illustrating the concentrating process of $CaSO_4$ solution with NaCl additive in membrane modulus, where flow conditions can be characterized by $\tau_{99\%}$ = 1,000 s (where the initial 384 s is dedicated for actual working section (*A*)). Analyzing these data one concludes, that for identical inlet conditions (C_{in} = 0.01 mol $CaSO_4$/dm³, C_{NaCl} = 0.22 mol/dm³) systematic increase in membrane separation process intensity, represented directly by dC/dt, results in a better effect – higher

outlet concentration of retentate, C_{out}. Nevertheless, an increase in dC/dt parameter value is simultaneously responsible for the rise of maximal attainable (however, without spontaneous nucleation) final concentration, C_{max}. For the first case (No. 1) final, outlet concentration of retentate is within the undersaturated region, thus work conditions are fully safe. But this case seems to be uneconomical since the low effect of concentration increment may be unacceptable. Higher dC/dt are thus demanded, which require rather precise counterbalancing between process safety and the economy rules. In particular, the C_{out} must be within the metastable zone, namely, be higher than saturation C^* and lower than the labile region boundary represented by C_{max}. Analyzing the data in Table 1, it results, that only No. 2–6 cases fulfill this requirement. One can also notice, that depending on dC/dt (0.2–0.6 mol/(dm³ h)) parameter the maximal, but still permissible residence time of retentate is within the 69,915–949 s range. The final concentration of retentate C_{out} reaches ca. 46.7%–94.6% of the maximal level, thus the first condition seems to be fulfilled. The total acceptable time, however, covers worktime (the initial 384 s) in the actual membrane suction section (*A*) and induction time in the outlet section (*B*), where further concentration increment is not possible while the existing, accumulated supersaturation is the subject of more or less spontaneous discharge. Since specific process hydrodynamics and spatial arrangement of membrane module provide in this case $\tau_{99\%}$ = 1,000 s, only No. 2–5 can be considered safe. This is the second limiting condition of safe operation. In case of No. 6, the maximal acceptable residence time 949 s (= 384 s in (*A*) + 565 s in (*B*) section) is shorter than the $\tau_{99\%}$ = 1,000 s, thus spontaneous nucleation before safe removal of the 99% of final retentate from the membrane module construction is expected. The case No. 5 appears to be safer, permitting to reach only ca. 83.5% of the possible concentration level, but avoiding spontaneous nucleation.

For the other cases (No. 7–10 in Table 1) it is predicted from the model, that concentration of retentate with dC/dt 0.7–1.0 mol/(dm³h) through 384 s provides final concentration C_{out} representing ca. 105%–134% of maximally attainable level, appropriately. Spontaneous precipitation is expected even within the actual working section of membrane module (*A*), responsible thus for scaling effects. In these cases (No. 7–10) some engineering intervention should be done during the design stage – preferably by shortening the residence time in suction section (*A*) of the membrane module. Simulated results of such engineering corrections are presented as No. 7a–10a. Instead of original 384 s work time, the values from within the 210–310 s range are relatively precisely predicted and recommended, resulting in decreased C_{out} values which are now within the safe (ca. 78.7%–87.4%) range. These correspond to induction times (resulting directly from the final C_{out}) from within the 754–946 s range and maximal permissible residence times from 1,041 to 1,176 s, advantageously slightly longer than $\tau_{99\%}$ = 1,000 s, thus spontaneous nucleation within membrane module construction can be avoided.

In Table 2, there are presented the results corresponding to different membrane module type providing in effect $\tau_{99\%}$ = 500 s (where the initial 198 s is dedicated for section (*A*)). Different residence time distribution, quantified

shortly as $\tau_{99\%}$, may result, for example, from a specific combination of general module geometry, diversified spatial arrangement of spacers, their shape(s), spacer interconnections template, overall module length, volumetric flow rate of feed/retentate, its composition (concentrations, ratios of the components, etc.), process temperature responsible for fluid density, viscosity, diffusivity, and other factors. In this technological case first three approaches (No. 1–3) are safe since undersaturated final retentate is removed. But these cases are rather strongly uneconomical – final concentrations of retentate are too low, these are even located outside the metastable zone. Under the examined hydrodynamic conditions (module geometry with flow intensity) the $\tau_{99\%}$ = 500 s, thus all other cases (No. 4–10) appears to be safe since the corresponding maximal permissible residence time varies from 61,996 to 1,366 s, what corresponds to systematically raised process intensity represented by dC/dt from 0.4 up to 1.0 mol/(dm³ h).

Analyzing the data presented graphically in Figs. 3 and 4 one can notice, that increase in final retentate concentration C_{out} corresponds to significant, non-linear shrinkage of induction time (especially it is visible in Fig. 4, where induction time is presented directly, whereas in Fig. 3 – as the log data – diffusing slightly the non-linear effects). Co-presence of NaCl, increasing gypsum solubility, may be regarded to be a factor slightly elongating this time, thus stabilizing the system against the spontaneous discharge of the accumulated supersaturation, directly leading to the spontaneous nucleation, and scaling phenomena. Effect of NaCl concentration is the most significant for relatively lower final retentate concentration (0.09 mol/dm³). An increase in C_{out} makes, that the stabilizing effect of NaCl is less pronounced, thus variation with induction time resulting from various NaCl doses is less visible.

The data from Tables 1–2 are also presented in Figs. 5 and 6, where economical/safe regions are marked. It is worth to note, that these regions simultaneously represent lower (intersection of $C_{out} = f(dC/dt)$ and C^* = const. dependencies) and upper (intersection of $C_{out} = f(dC/dt)$ and $C_{max} = f(dC/dt)$ dependencies) limits of the metastable zone. Retentates from these regions are supersaturated, thus economic criteria are fulfilled, however, are still within the relatively safe metastable region, where supersaturation is not expected to discharge spontaneously. Under the conditions presented in Fig. 5 (Table 1) the region has both right and left boundaries. Contrary, in the case of Fig. 6 (representing the data from Table 2) only lower boundary is presented, thus the possible disadvantageous shift into the labile region – under these specific process conditions – is not expected anyway, guarantying thus safe membrane working conditions for a broader range of the dC/dt design parameter values.

For practical safe exploitation of these membrane modules one should remember, that higher membrane concentrating yield corresponds to higher C_{out} values, but always $C_{out} < C_{max}$ must be fulfilled. Smaller deviation of C_{out} from C_{max} provides shorter induction times, which – in turn – must be also always higher than the time necessary for safe transportation of the retentate from "danger zone," reflecting, however, the specific hydrodynamic environment at the membrane module outlet part.

For the presented simulations constant value of NaCl concentration (C_{NaCl} = 0.22 mol/dm³) was used for simplification. In a real process, C_{NaCl} may also vary depending on the current chemical composition of the processed retentate. Thus, what should be emphasized, the very idea of the design method is retained, while to increase the accuracy of calculations, the module should be conventionally divided into a larger number of smaller segments, and for each of them the mass balances of the ions should be done (including the selectivity of the membrane separation process) while the C^* and C_{max} values updated on this basis (especially in respect to the current value of C_{NaCl}) can be employed.

Nevertheless, the possible gradual increase in the concentration of NaCl during the retentate concentration process (Fig. 1) increases the maximum supersaturation values C_{max} in this system, hence the assumption of a constant value of C_{NaCl} for the entire process applied in this study does not affect the security of design prediction, increasing only the safety range of the process calculations.

5. Conclusions

Economical and simultaneously relatively safe work conditions of the membrane module are the important technological and engineering challenge. It may be achieved without any chemicals (antiscalants) addition. Instead, many technological and constructional factors must be considered and counterbalanced. Safe optimum with respect to final retentate concentration must be identified, matching economical rules, and technical flow stabilization (avoiding the formation of nuclei suspension, leading to membrane surface scaling).

The employed design equations and other dependencies can find them useful in various design calculations, where process conditions providing gypsum scaling delay or prevention must be arranged. These enable one to select such membrane working part's (A) length and/or concentrating intensification dC/dt, which – for a given combination of a feed composition used (C_{in}, C_{NaCl}) and established retentate flow characteristic (unique, given residence time distribution) – provide safe evacuation of ca. 99% of the post-processed retentate from the membrane system before unwanted nucleation/scaling phenomena occur. Practical design rules were provided, numerically verified, and interpreted based on simulation results.

The presented set of employed equations can be used as a "trial and error method," however in the future concept of some, more advanced calculation program can be presented, automatically providing some optimal concentration strategy based on a larger set of variables characterizing hydrodynamic conditions, feed properties, demanded final retentate quality, and suction intensity within the working section of the membrane. Moreover, some more complex scenarios can be simulated and thus rationally evaluated, considering, for example, the nonlinear profile of the suction intensity along with the membrane module, modification of C_{NaCl} along with the module, and deviations from the ideal plug-flow hydrodynamic regime in a membrane actual working sector (A).

Acknowledgments

Symbols

A	—	Working section of the membrane module
a	—	Parameter
B	—	Outlet section of the membrane module
C	—	Concentration, mol/dm³
C_{in}	—	Inlet concentration of the feed (at the module inlet), mol/dm³
C_{LBMZ}	—	Concentration of retentate representing lower boundary of the metastable zone (=C^*), mol/dm³
C_{max}	—	Maximal attainable supersaturation, mol/dm³
C_{NaCl}	—	Concentration of NaCl, mol/dm³
C_{out}	—	Final concentration of retentate (at termination of the membrane process), mol/dm³
C_{UBMZ}	—	Concentration of retentate representing upper boundary of the metastable zone, labile region's boundary, mol/dm³
C^*	—	Saturation concentration (solubility) of calcium sulfate in its aqueous solution for a given co-present NaCl concentration, C_{NaCl}, mol/dm³
k_N	—	Parameter
S	—	Relative supersaturation, = C_{out}/C^*
S_{crit}	—	Critical relative supersaturation, = C_{max}/C^*
t	—	Time, s
t_{ind}	—	Induction time, s
dC/dt	—	Concentrating rate, mol/dm³/h
σ	—	Standard deviation, s
τ	—	Mean residence time of retentate in a working volume of membrane module, s
$\tau_{99\%}$	—	Residence time of retentate corresponding to removal of 99% of the feed from the membrane module working volume, s

References

[1] A. Antony, J.H. Low, S. Gray, A.E. Childress, P. Le-Clech, G. Leslie, Scale formation and control in high pressure membrane water treatment systems: a review, J. Membr. Sci., 383 (2011) 1–16.

[2] M. Turek, K. Mitko, K. Piotrowski, P. Dydo, E. Laskowska, A. Jakóbik-Kolon, Prospects for high water recovery membrane desalination, Desalination, 401 (2017) 180–189.

[3] D.M. Warsinger, J. Swaminathan, E. Guillen-Burrieza, H.A. Arafat, J.H. Lienhard V, Scaling and fouling in membrane distillation for desalination applications: a review, Desalination, 356 (2015) 294–313.

[4] B. Tomaszewska, E. Kmiecik, K. Wątor, M. Tyszer, Use of numerical modelling in the prediction of membrane scaling: reaction between antiscalants and feedwater, Desalination, 427 (2018) 27–34.

[5] F.H. Butt, F. Rahman, U. Baduruthamal, Identification of scale deposits through membrane autopsy, Desalination, 101 (1995) 219–230.

[6] M. Xie, C.Y. Tang, S.R. Gray, Spacer-induced forward osmosis membrane integrity loss during gypsum scaling, Desalination, 392 (2016) 85–90.

[7] C.A.C. van de Lisdonk, J.A.M. van Paassen, J.C. Schippers, Monitoring scaling in nanofiltration and reverse osmosis membrane systems, Desalination, 132 (2000) 101–108.

[8] C.A.C. van de Lisdonk, B.M. Rietman, S.G.J. Heijman, G.R. Sterk, J.C. Schippers, Prediction of supersaturation and monitoring of scaling in reverse osmosis and nanofiltration membrane systems, Desalination, 138 (2001) 259–270.

[9] A.J. Karabelas, A. Karanasiou, S.T. Mitrouli, Incipient membrane scaling by calcium sulfate during desalination in narrow spacer-filled channels, Desalination, 345 (2014) 146–157.

[10] E. Lyster, J. Au, R. Rallo, F. Giralt, Y. Cohen, Coupled 3-D hydrodynamics and mass transfer analysis of mineral scaling-induced flux decline in a laboratory plate-and-frame reverse osmosis membrane module, J. Membr. Sci., 339 (2009) 39–48.

[11] M. Turek, K. Mitko, P. Dydo, K. Piotrowski, E. Laskowska, A. Jakóbik-Kolon, New Approach to the Membrane Scaling Risk Assessment, Proceedings of IDA World Congress 2017, Water Reuse and Desalination, Sao Paulo, Brasil, IDAWCREF: 17WC-57879, 2017.

[12] M. Turek, P. Dydo, J. Waś, Electrodialysis reversal in high CaSO₄ supersaturation mode, Desalination, 198 (2006) 288–294.

[13] M. Turek, J. Waś, K. Mitko, Scaling prediction in electrodialytic desalination, Desal. Water Treat., 44 (2012) 255–260.

[14] M. Turek, K. Mitko, Residence time distribution of the electrodialyzer under electric field conditions, Desalination, 342 (2014) 139–147.

[15] P. Dydo, M. Turek, J. Ciba, Laboratory RO and NF processes fouling investigation by residence time distribution curves examination, Desalination, 164 (2004) 33–40.

[16] D. Hasson, A. Drak, C. Komlos, Q. Yang, R. Semiat, Detection of fouling on RO modules by residence time distribution analyses, Desalination, 204 (2007) 132–144.

[17] P. Dydo, M. Turek, J. Ciba, K. Wandachowicz, J. Misztal, The nucleation kinetic aspects of gypsum nanofiltration membrane scaling, Desalination, 164 (2004) 41–52.

[18] D. Hasson, A. Drak, R. Semiat, Induction times induced in an RO system by antiscalants delaying CaSO₄ precipitation, Desalination, 157 (2003) 193–207.

[19] F. Alimi, H. Elfil, A. Gadri, Kinetics of the precipitation of calcium sulfate dihydrate in a desalination unit, Desalination, 157 (2003) 9–16.

[20] D.M. Warsinger, E.W. Tow, J. Swaminathan, J.H. Lienhard V, Theoretical framework for predicting inorganic fouling in membrane distillation and experimental validation with calcium sulfate, J. Membr. Sci., 528 (2017) 381–390.

[21] N. Pomerantz, Y. Ladizhansky, E. Korin, M. Waisman, N. Daltrophe, J. Gilron, Prevention of scaling of reverse osmosis membranes by "zeroing" the elapsed nucleation time. Part I. calcium sulfate, Ind. Eng. Chem. Res., 45 (2006) 2008–2016.

[22] A. Lancia, D. Musmarra, M. Prisciandaro, Measuring induction period for calcium sulfate dihydrate precipitation, AIChE J., 45 (1999) 390–397.

[23] D.M. Keller, R.E. Massey, O.E. Hileman Jr., Studies on nucleation phenomena occurring in aqueous solutions supersaturated with calcium sulfate. II. The induction time, Can. J. Chem., 56 (1978) 3096–3103.

[24] F. Alimi, A. Gadri, Kinetics and morphology of formed gypsum, Desalination, 166 (2004) 427–434.

[25] I.J. Reznik, I. Gavrieli, J. Ganor, Kinetics of gypsum nucleation and crystal growth from Dead Sea brine, Geochim. Cosmochim. Acta, 73 (2009) 6218–6230.

[26] M.M. Tlili, P. Rousseau, M. Ben Amor, C. Gabrielli, An electrochemical method to study scaling by calcium sulphate of a heat transfer surface, Chem. Eng. Sci., 63 (2008) 559–566.

[27] E. Barbier, M. Coste, A. Genin, D. Jung, C. Lemoine, S. Logette, H. Muhr, Simultaneous determination of nucleation and crystal growth kinetics of gypsum, Chem. Eng. Sci., 64 (2009) 363–369.

[28] F. Rahman, Calcium sulfate precipitation studies with scale inhibitors for reverse osmosis desalination, Desalination, 319 (2013) 79–84.

[29] J. Benecke, M. Haas, F. Baur, M. Ernst, Investigating the development and reproducibility of heterogeneous gypsum scaling on reverse osmosis membranes using real-time membrane surface imaging, Desalination, 428 (2018) 161–171.

AQ1

[30] M. Uchymiak, E. Lyster, J. Glater, Y. Cohen, Kinetics of gypsum crystal growth on a reverse osmosis membrane, J. Membr. Sci., 314 (2008) 163–172.

[31] D.L. Shaffer, M.E. Tousley, M. Elimelech, Influence of polyamide membrane surface chemistry on gypsum scaling behavior, J. Membr. Sci., 525 (2017) 249–256.

[32] M. Shmulevsky, X. Li, H. Shemer, D. Hasson, R. Semiat, Analysis of the onset of calcium sulfate scaling on RO membranes, J. Membr. Sci., 524 (2017) 299–304.

[33] S.B. Ahmed, M.M. Tlili, M. Amami, M.B. Amor, Gypsum precipitation kinetics and solubility in the NaCl-MgCl$_2$-CaSO$_4$-H$_2$O system, Ind. Eng. Chem. Res., 53 (2014) 9554–9560.

[34] E.W. Mockobey, The Solubility of Calcium Sulfate in Sodium Chloride Solutions, Master Thesis, Missouri University of Science and Technology, Curtis Laws Wilson Library, 1932.